(18)
(12)
(2)

(6) STUDIES ON THE FAILURE OF METAL MECHANICAL JOINTS

SUBJECTED TO DYNAMIC LOADS.

(9) FINAL REPORT. 1 Oct 76 - 30 Sep 77,

(10) C. A. /ROSS,
R. L./SIERAKOWSKI
J. W./HOOVER

(11) 30 SEP 1977

(13) 46p.

U.S. AIR FORCE OFFICE OF SCIENTIFIC RESEARCH

(15)
GRANT NUMBER, ✓ AFOSR-76-3157

(16) 2397

(17) B1

UNIVERSITY OF FLORIDA, Eglin AFB
Graduate Engineering Center,

D D C
RECEIVED
FEB 13 1978
B

407 525

REPORT DOCUMENTATION PAGE	READ INSTRUCTIONS BEFORE COMPLETING FORM

1. REPORT NUMBER	2. GOVT ACCESSION NO	3. RECIPIENT'S CATALOG NUMBER
AFOSR-TR- 78 - 0 0 7 8		

4. TITLE (and Subtitle)	5. TYPE OF REPORT & PERIOD COVERED
STUDIES ON THE FAILURE OF METAL MECHANICAL JOINTS SUBJECTED TO DYNAMIC LOADS	FINAL 1 Oct 76 - 30 Sep 77
	6. PERFORMING ORG. REPORT NUMBER

7. AUTHOR(s)	8. CONTRACT OR GRANT NUMBER(s)
C A ROSS R L SIERAKOWSKI I W HOOVER	AFOSR 76-3157 new

9. PERFORMING ORGANIZATION NAME AND ADDRESS	10. PROGRAM ELEMENT, PROJECT, TASK AREA & WORK UNIT NUMBERS
UNIVERSITY OF FLORIDA GRADUATE ENGINEERING CENTER, PO BOX 1918 EGLIN AFB, FL 32542	2307B1 61102F

11. CONTROLLING OFFICE NAME AND ADDRESS	12. REPORT DATE
AIR FORCE OFFICE OF SCIENTIFIC RESEARCH/NA BLDG 410 BOLLING AIR FORCE BASE, D C 20332	Sep 77
	13. NUMBER OF PAGES
	43

14. MONITORING AGENCY NAME & ADDRESS(if different from Controlling Office)	15. SECURITY CLASS. (of this report)
	UNCLASSIFIED
	15a. DECLASSIFICATION/DOWNGRADING SCHEDULE

16. DISTRIBUTION STATEMENT (of this Report)

Approved for public release; distribution unlimited.

D D C
RECEIVED
FEB 16 1978
B

17. DISTRIBUTION STATEMENT (of the abstract entered in Block 20, if different from Report)

18. SUPPLEMENTARY NOTES

19. KEY WORDS (Continue on reverse side if necessary and identify by block number)

RIVETED JOINTS   RIVET LOADS
BLAST LOADING
DYNAMIC LOADING
RIVETED PANELS
STRESS CONCENTRATIONS

20. ABSTRACT (Continue on reverse side if necessary and identify by block number)

A series of experimental dynamic tests were conducted on riveted joints and struts with central holes to establish quantitatively fracture mechanisms and to determine dynamic load factors based on measured strains. Results of these experimental tests on aluminum struts with a central circular indicate that dynamic stress concentrations associated with the hole are approximately equal to the static stress concentrations for the same specimen. Riveted joints subjected to dynamic loadings exhibit the same general fracture/failure modes associated with similarly static loaded riveted joints. Dynamic response of riveted joints and subsequent fracture is very dependent on the joint stiffness and loading history

DD FORM 1473 EDITION OF 1 NOV 65 IS OBSOLETE

ii

FOREWORD

The work reported herein was performed under joint sponsorship by the Air Force Office of Scientific Research, Bolling AFB, D. C. 20332 and the Air Force Armament Laboratory, Eglin AFB, FL 32542, under grant number AFOSR 76-3157. Mr. William J. Walker, AFOSR/NA, was the Air Force Program Manager.

The results described in this final scientific report summarize the technical effort accomplished in the period from October 1, 1976 through September 30, 1977.

The work was performed by the University of Florida Graduate Engineering Center, Eglin AFB, FL 32542 and the Engineering Science Department, University of Florida, Gainesville, FL 32611. University of Florida personnel who contributed to this study were C. A. Ross, R. L. Sierakowski and J. W. Hoover. Grateful acknowledgement is made to W. S. Strickland, AFATL/DLYV, Eglin AFB, FL 32542, for his technical assistance and cooperation in the full scale tests.

PRECEDING PAGE BLANK-NOT FILMED

TABLE OF CONTENTS

LIST OF FIGURES

LIST OF FIGURES (Continued)

LIST OF TABLES

SECTION I

INTRODUCTION

The principal requirement of any structural component
when used in a complex structural system is to insure that
the structural configuration remain intact when subjected to
the static and dynamic design loads. This necessitates an
understanding of the load transfer mechanism between and with-
in structural components, and more importantly the load transfer
mechanisms at the attachment points between adjacent components.
In order to identify attachment or joining techniques, two very
broad classes can be inferred as being either of the bonded and/
or mechanical joint types. To differentiate between these two
classes, the mechanical joints will be defined herein as those
requiring a cutout or hole in the parent material for placement
of the fastener. The absence of this removed material reduces
the potential useful component strength below that of the tested
ultimate strength of the material. In addition the very nature
of the type of loading is found to play an important role in
characterizing the observed resultant attachment fracture.
Fracture in this case and as used in this study is defined as
actual material rupture or seperation of one part of the attach-
ment from the other.

The general fabrication schemes of aerospace vehicles re-
quires the use of various attachment types particularly in

1.

semi-monocoque construction. In the present investigation, primary attention has been focused on one attachment type, that of mechanical riveted connections found typically in sheet-stiffener combinations of semi-monocoque structures. To examine previous work on this subject, an extensive literature review was conducted which included literature searches of DOD files, NASA files, open literature and in progress research by Eglin AFB Technical Library, North Carolina State Science and Technology Research Center, Naval Research Laboratory Shock and Vibration Information Center. These literature searches have revealed that little if any information exists on failure mechanics of dynamically loaded riveted joint assemblies. In view of this paucity of information, the present investigative approach has been to initiate a study into establishing qualitatively mechanisms of fracture for dynamically loaded riveted joint assemblies and to determine dynamic load factors based on measured strains at near field and far field positions relative to the rivets. To obtain this information, a series of experiments were conducted on various sheet-rivet combinations and struts containing a single hole, using a drop weight device. In additon full scale blast loaded instrumented panels were tested in cooperation with the USAF Armament Laboratory, Eglin AFB, Florida.

The experimental tests and results are described and discussed in detail in Section II. A detailed plate analysis and test results as obtained in the full scale tests are given in Section III, with conclusions and recommendations for further study given in Section IV.

SECTION II

EXPERIMENTAL TESTS AND DISCUSSION

2.1 INTRODUCTION

Several variations of a drop weight test using the device
shown in Figure No. 1 were conducted using both simple sheet
and riveted specimens containing a central circular hole or
rivet. The material used for all test specimens was 2024-T3 alumi-
num alloy sheet. All rivets used in the fabrication of these
specimens were made from 2117-T4 aluminum alloy material. Both
Baldwin Lima Hamilton (BLH) and Micro-Measurements (MM) resistance
foil strain gages were used in these tests.

In additon to the laboratory tests above, a series of full
scale field tests were conduc.ed in cooperation with the USAF
Armament Laboratory. These tests consisted of using 68.5 x 62.9 cm
2024-T3 aluminum alloy panels riveted along all edges with
various rivet patterns and sizes in order to obtain information
on rivet/sheet fracture mechanisms under blast loadings. These
blast loaded panels were instrumented using foil resistance
strain gages as noted above.

2.2 STRUTS WITH CENTRAL HOLE

The influence of static stress concentration factors for an
infinitely wide plate with a circular hole as shown in Figure 2

4.

121.9cm

1.27cm Drill Rod

Holding Fixture Using
.953cm Diameter Bolt
To Hold Specimen

Specimen

17.78cm

1.27cm Drill Rod

Drop Weight
Three Different Sizes
1. 15.24cm long steel
2. 30.48cm long steel
3. 30.48cm long lead

121.9cm
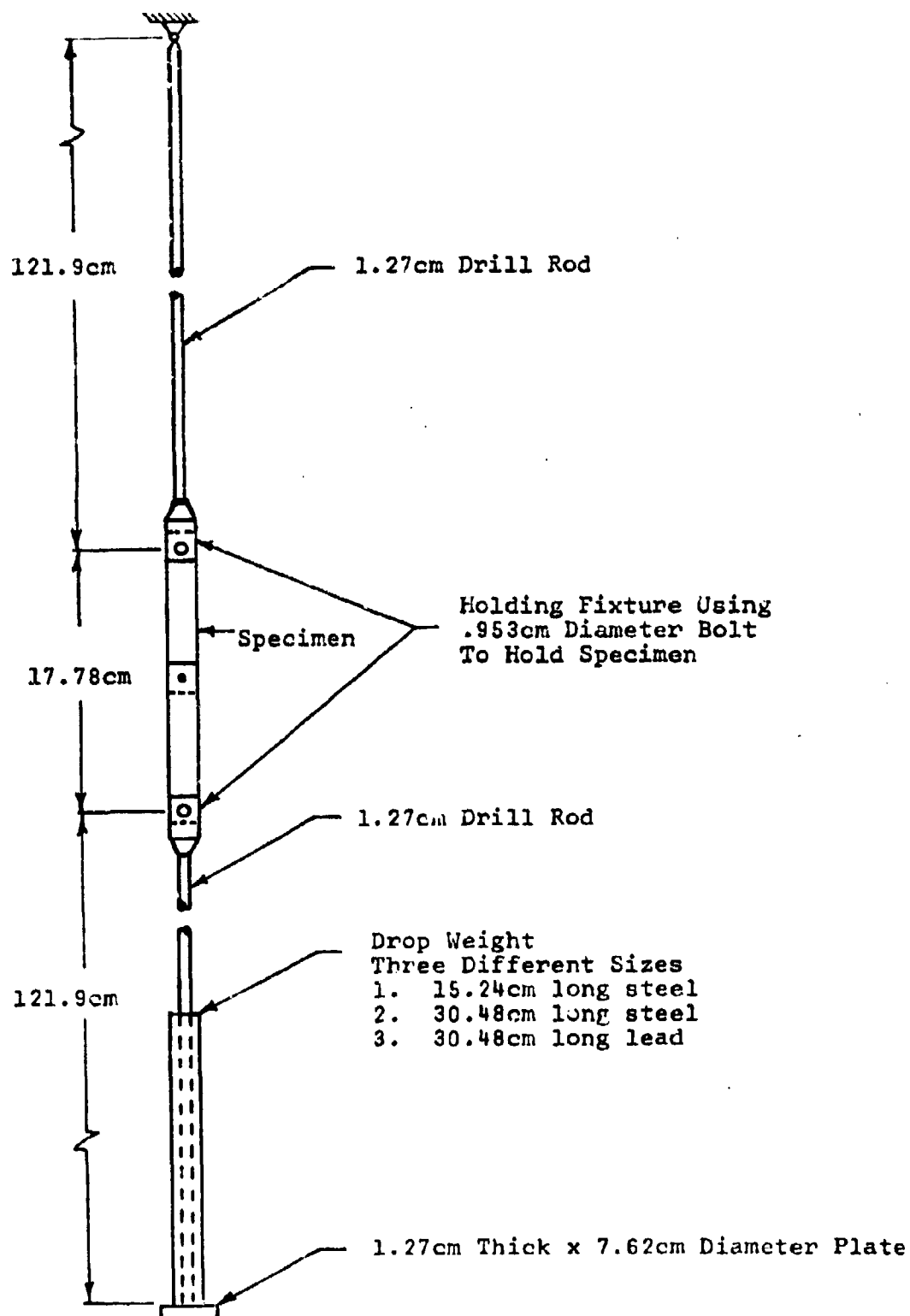
1.27cm Thick x 7.62cm Diameter Plate

Figure 1. Drop Weight Device Used in Various Tests.

5.

has been discussed in detail in such classical elasticity texts as Timoshenko (Reference 1) and the general solution is given graphically in Figure 3. The effect of decreasing specimen width is to cause an increase in the maximum static stress concentration factor at the edge of the hole. However, it has been shown by Peterson (Reference 2) that for a radius/width (a/w) ratio up to 0.25 the maximum static stress concentration factor is only 1.0% greater than that for a plate of infinite width, that is, a/w = 0.

To form a basis for comparison with later tests, a series of tests are described in this section which are based upon the assumption that if dynamic stress concentrations are inherently different from those found in static loadings then these differences would be evident in strain measurements around a circular hole in a thin strut when subjected to a dynamic load. Stress concentration factors for dynamic loadings have been determined experimentally by Dally (References 3 and 4) for struts of birefringent material with central circular holes. The struts of References 3 and 4 were loaded in a device similar to that of Figure 1 and fringe patterns using flash photography and photo-elastic equipment were recorded. The results of Dally's experiments show that the dynamic stress concentration factor, defined in the same fashion as in Figures 2 and 3, was approximately equal to or slightly less than the static value reported in Petersen (Reference 2).
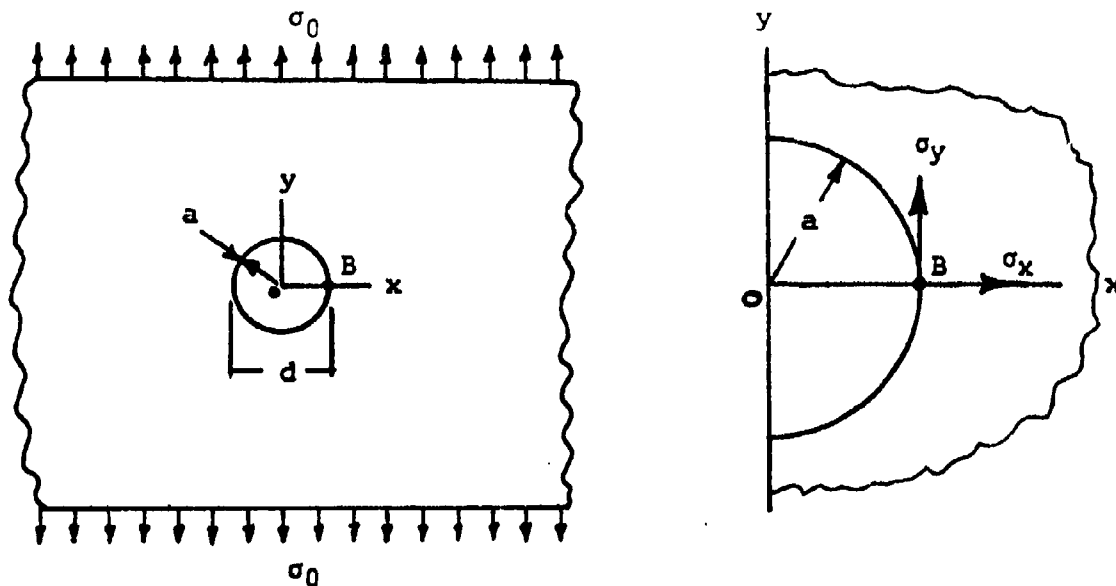
6.

Figure 2. Circular Hole in Flat Plate of Infinite Width with Applied Far Field Stress σ_0.
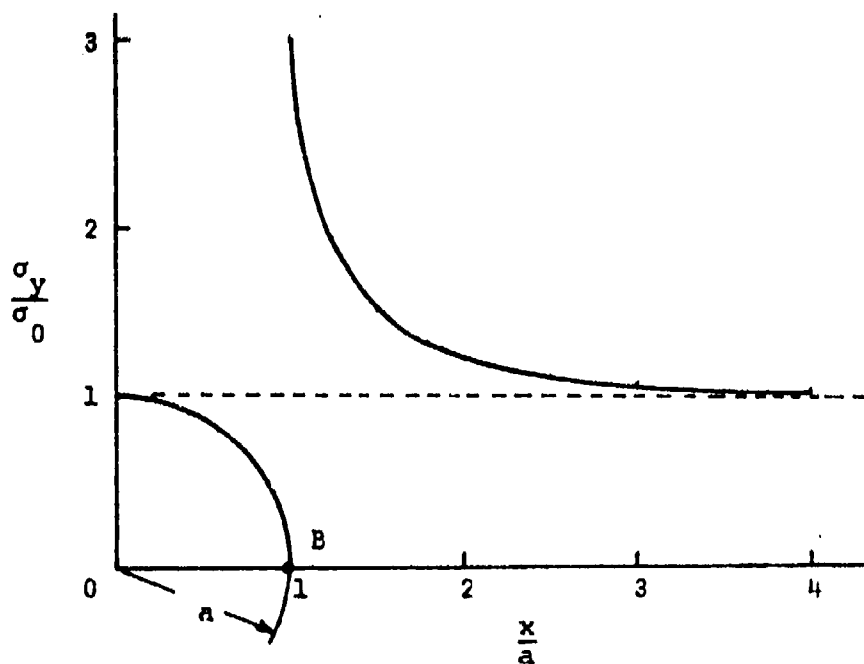

Figure 3. Ratio of Stress (Stress Concentration Factor) Along Bx for Plate Shown Figure 2.

7.

In the present study a series of tests as described above
for birefringent materials were conducted on 2024-T3 aluminum
alloy specimens as shown in Figure 4. High elongation foil re-
sistance strain gages, (type MM EP-08-031AP-120), with a .079 cm
width grid were trimmed as narrow as possible and placed adjacent
to the hole. The positions of gages 2 and 3 relative to the
adjacent hole were determined after gage installation. Strains
were recorded on a multi-channel recorder with the maximum
strains noted for each gage for analysis purposes. The ratios
of strains in gages 2 and 3 to that of gage 1 were calculated and
the results are plotted in Figure 5. The solid line of Figure 5
represents the analytical expression of Reference 1 corrected
for width effect while the open circles represent ratios deter-
mined from the dynamic drop tests and the solid circles represent
ratios for the same kind of specimen determined from static
tests. The dynamic data represents the results of over 30 tests
using two different size specimens and three different sizes of
drop weights. For basic reference, the strains at gage position
1 are shown as a function of drop height in Figure 6. Static
data was also taken on similar type specimens as tested in tension
in a tensile test machine. The overall results for these tests
show that there appears to be very little difference between the
value of the static stress concentration as compared to the
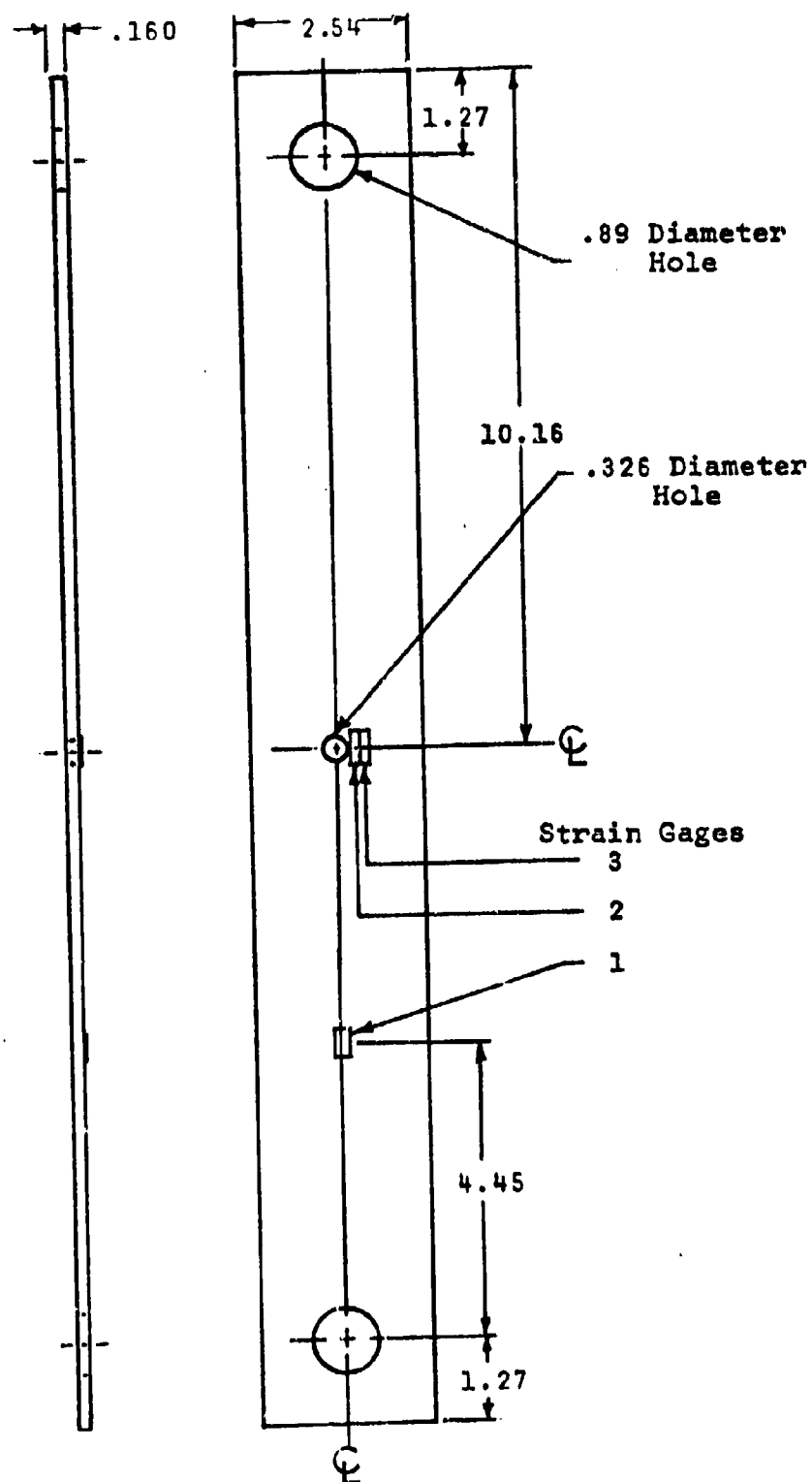
8.

Figure 4. Strut with Central Hole used for Determining Dynamic Stress Concentrations. All Dimensions in Centimeters.
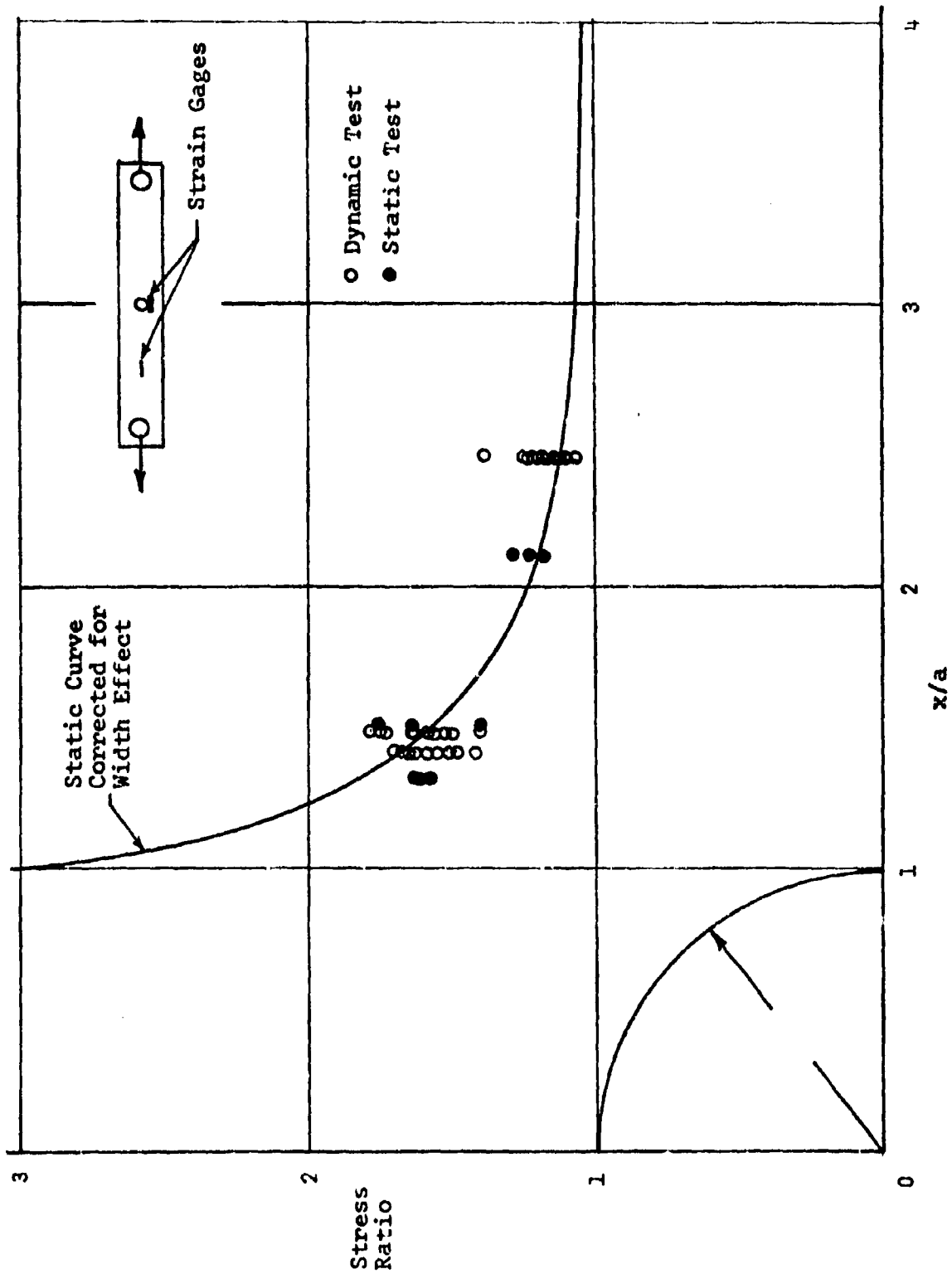
Figure 5. Stress Concentration Factors for Specimen Shown in Figure 4. Stress Ratio Same as Shown in Figures 2 and 3.

10.
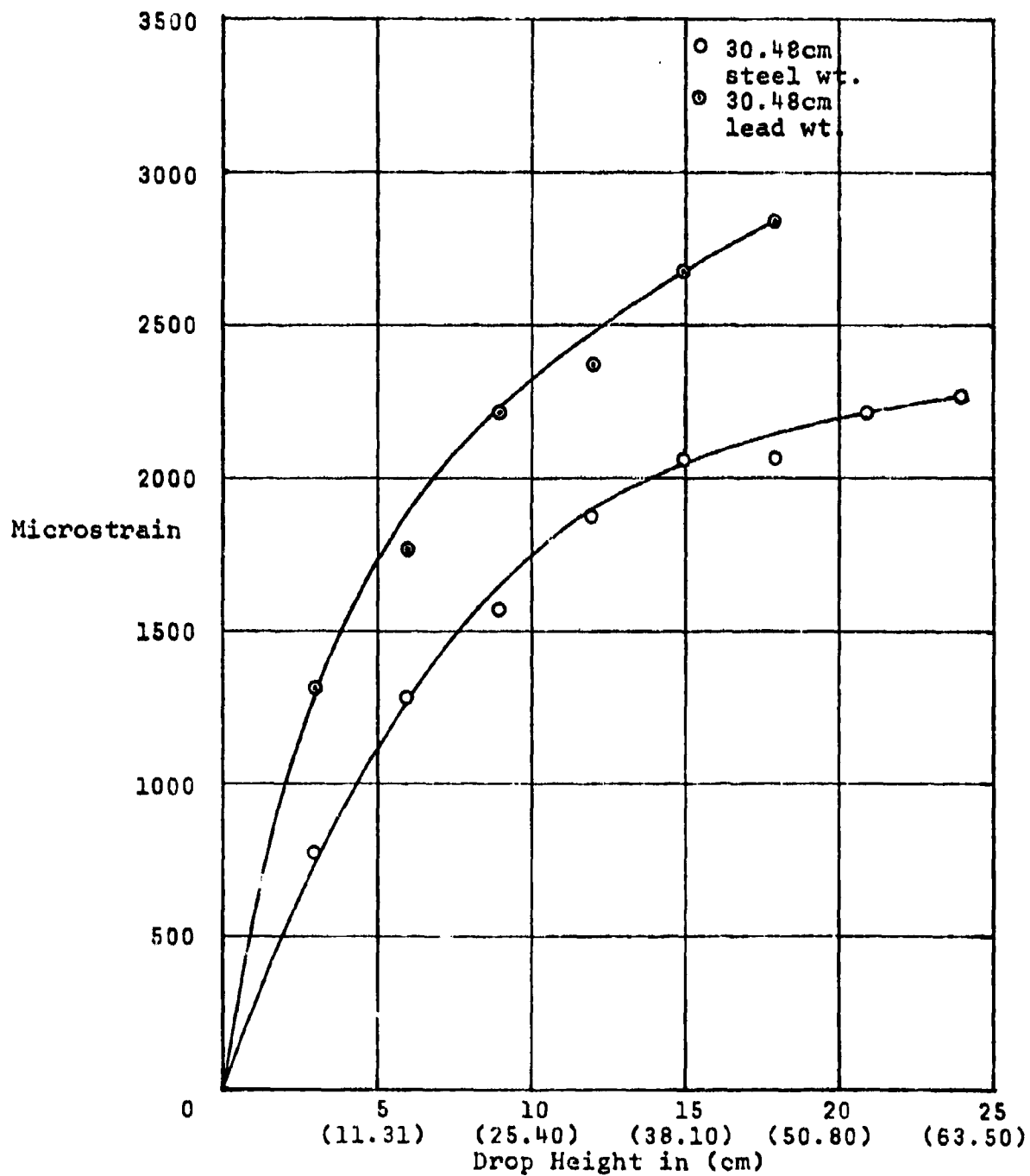
Figure 6. Maximum Strain as Function of Drop Height for Two
Different Drop Weights. Specimen shown in Figure 4.
Strains Measured at Gage 1.

11.

dynamic stress concentration, thereby reaffirming the results
of Dally (References 3 and 4).

2.3 RIVETED JOINTS

For the riveted joint assemblies, a series of tests as
shown in Figure 7 and as fabricated according to the specifica-
tions of MIL-STD-1312, were conducted. These tests were conducted
in order to determine qualitatively rivet/sheet fracture mecha-
nisms and to quantitatively establish stress concentration factors
for single rivet specimens. All the specimens were tested in the
drop weight device as shown in Figure 1.

Classically, static loaded rivet/sheet combinations fail in
the sheet by anyone of the several failure modes as shown in
Figure 8. In addition to these sheet fracture modes a rivet
shear fracture is considered to be a major failure mechanism.
Static fracture loads for rivets can be calculated for protrud-
ing head rivet/sheet combination using the material properties
of the rivet and sheet, however for flush head rivets which are
countersunk or for dimpled sheets the fracture loads must be
determined experimentally and some widely accepted results are
tabulated in Reference 5.

In order to observe rivet fracture on a particular class of
rivets and attachment type and in order to quantify fracture
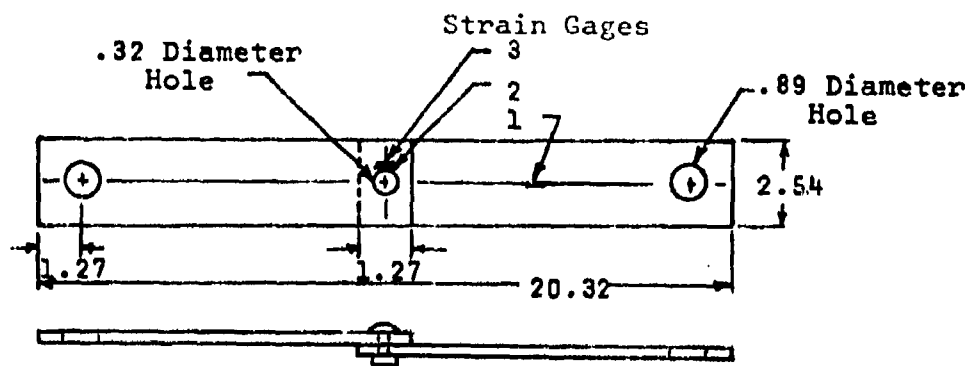
a) Single Lap Specimen.
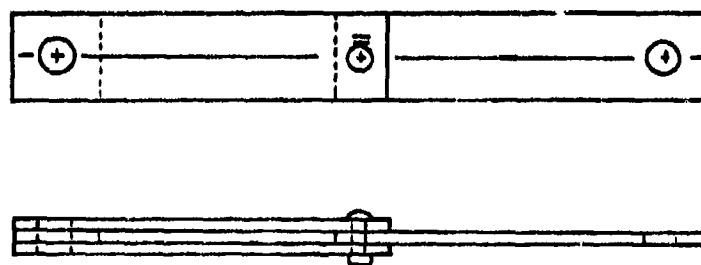
b) Double Lap Specimen

Figure 7. Single Rivet Spt mens Used in Drop Weight Tests. Same Dimensions i Flush Head Specimens. All Dimensions in Centimeters.
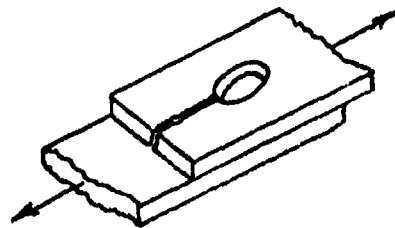
Bearing Failure   Cleavage Fracture
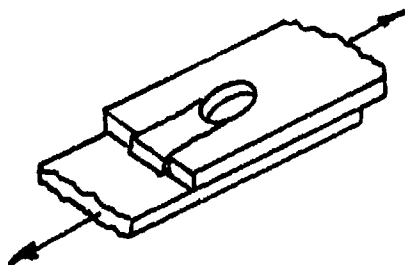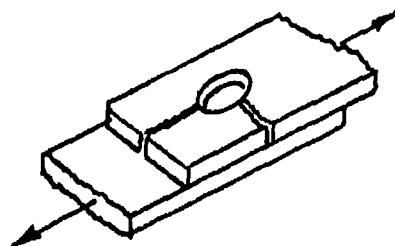
Shear Out Fracture   Combination Fracture
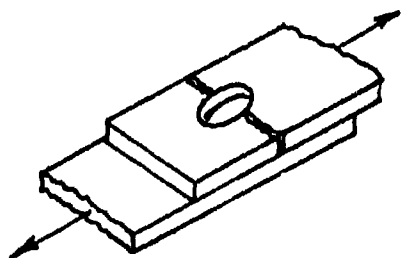
Net Tension Fracture   Shear Tear Out Fracture
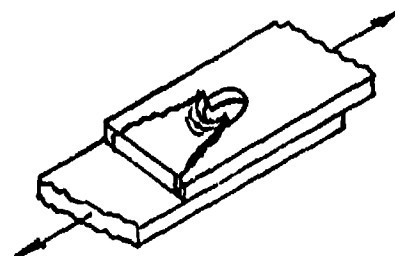
Figure 8.   Rivet Failure/Fracture Modes for Static Loads.

loads a series of drop weight tests were performed on counter-
sunk flush head rivets using both single and double shear specimens.
Aluminum alloy 2024-T3 sheet (.063 in (.16 cm) thick) with MS20-
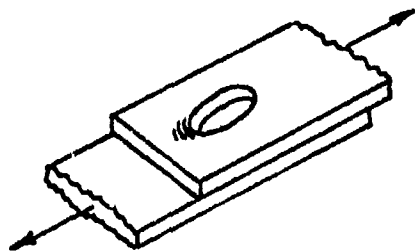426-AD4 rivets were used to fabricate all specimens tested. The
specimens were instrumented using foil resistance strain gages
as shown in Figure 6, and a drop weight of 2.48 kg with nominal
dimensions of 3.8 cm diameter by 30.5 cm long containing a 1.27
cm diameter central hole. The loads were successively applied
for these tests, that is, if the first drop height did not
fracture the specimen, then the next drop height was used until
failure occurred. The initial drop height used was 1 in (2.54 cm)
and increased by increments of 1 in (2.54 cm) until fracture
occurred. Rivet shear was always the observed fracture mode for
all tests, however considerable rivet rotation, about an axis
in the plane of the sheet, occurred prior to rivet shear.

Some typical strain readings, taken for the three gage
positions as shown in Figure 7, are shown in Figure 9. Gen-
eral observations indicated that considerable rivet rotation
and local bending of the sheet takes place before the rivet
fracture. The local bending appears to be more severe in
the immediate vicinity of the rivet and bending appears re-
duced at distances removed from the rivet. This is indicated
by the differences in the gage readings shown by the curves of
Figure 9. Also as the drop height is incrementally increased

15.
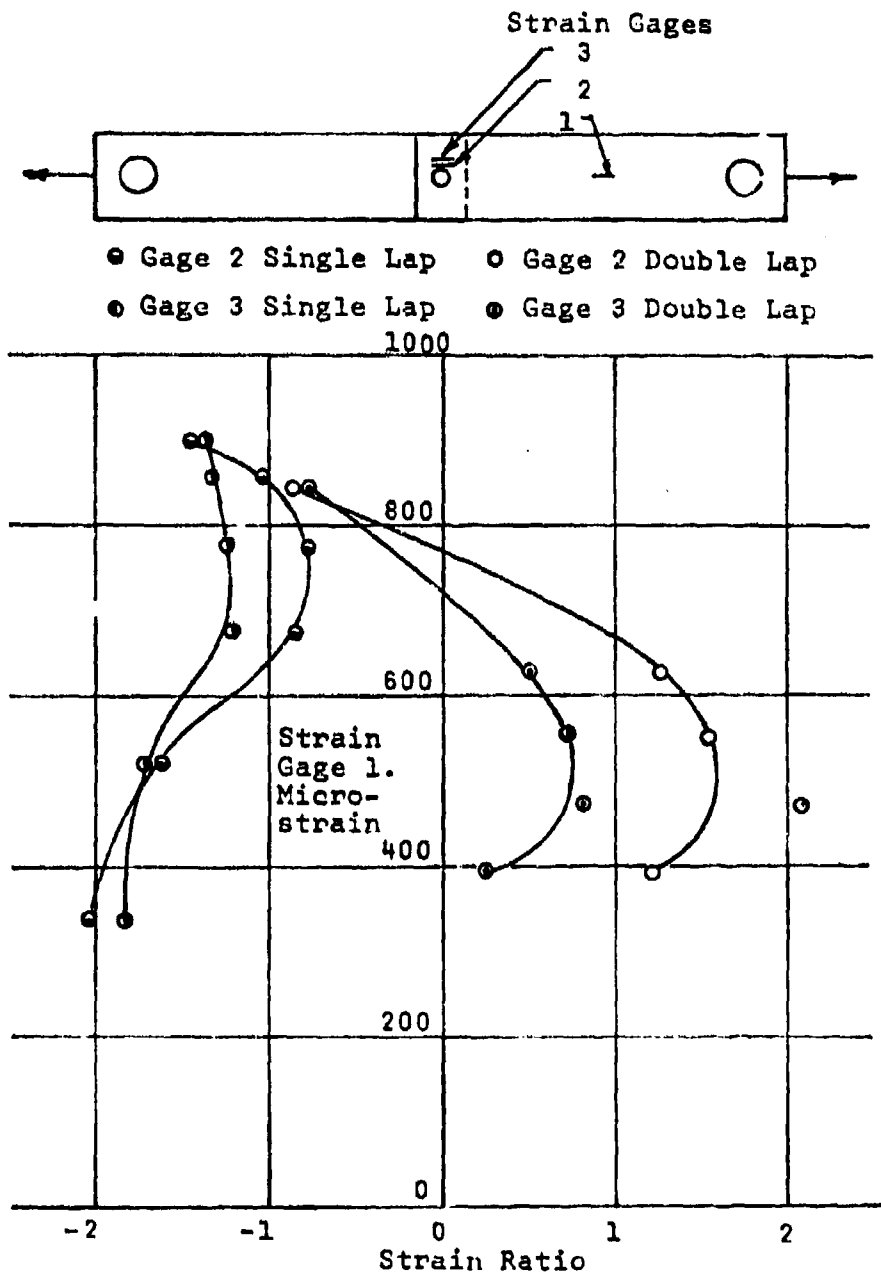
Figure 9. Strain Ratios for Lapped Flush Head Riveted Specimens
Vs Strain at Gage 1.

16.

there is a tendency for the bending to be reduced but further
increase in drop height increases the bending as shown by the
tendency of the curves to become more negative. This phenomenon
occurs in both the single and double lapped joints as evidenced
in Figure 9.

In addition to the flush head rivet tests a series of tests
using button head rivets of the type MS20-430-AD4 with 2024-T3
aluminum alloy sheet of varying thickness were conducted to
quantify the maximum fracture load as a function of sheet thick-
ness for a constant rivet diameter. Sheet thicknesses of .025,
.050 and .063 in(.064, .127, .160 cm) were used to fabricate
single lap specimens as shown in Figure 7a. Foil resistance
strain gages were applied back to back along the centerline of
one strip of the specimen, 1.0 in (2.54 cm) from rivet center line
as shown in Figure 7. Initial tests were performed on several
uninstrumented specimens to determine the drop height necessary
to produce fracture using the 12 in (30.48 cm) steel drop weight.
Instrumented specimens were then tested at the drop height re-
quired to produce fracture and the strains recorded. The maximum
strains and stresses at the drop heights necessary to produce
fracture are listed in Table I.

Tests performed on riveted specimens with both strips of
the specimen of the same thickness such as those in Table I
show symmetrical rotation and bending about a transverse axis

17.

TABLE I

MAXIMUM STRESSES AND LOADS FOR MS20-430-AD4 RIVET AND 2024-T3 SHEET

Sheet Thickness in (cm)	Fracture Drop Ht. in (cm)	Maximum Strain, ϵ μ Units		Ave. Strain $(\epsilon_1 + \epsilon_2)/2$ μ Units	Ave. Max. Stress KPSI (MPa)	*Ave. Max. Load Lbs.	Type of Failure
		Gage 1	Gage 2				
.063(.160)	9.0(22.86)	636	213	925	9.71(66.97)	612	Rivet rotation followed by rivet shear
.040(.102)	10.0(25.40)	1144	1440	1292	13.57(93.59)	517	Rivet rotation followed by rivet shear
.032(.081)	14.0(35.56)	1768	2366	2067	21.70(149.66)	695	Rivet rotation, bearing yielding, and elongation of hole followed by rivet shear
.025(.064)	11.0(27.94)	1411	1454	1433	15.05(108.79)	376	Severe rivet rotation and bearing yielding followed by shear tear out

Gage 1

Gage 2

1.0 / (2.54)

MS20-430-AD4

Both Strips Same Size.
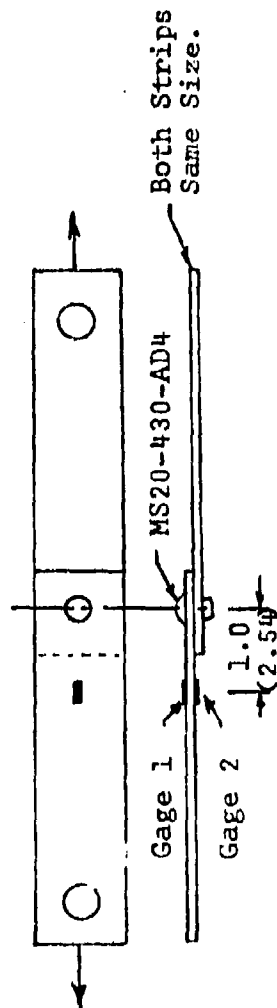
*Static shear fracture load for the rivet is 388 pounds

through the rivet centerline. In practical situations where the
sheet is attached to a stringer(s) or other stiffening members the
thicknesses of both structural elements need not be and generally
are not equal. In order to determine the effect of such thick-
ness differences between the two strips of the test specimen, a
.063 in (.160 cm) thick strip was riveted to sheet thicknesses
of .025, .032, and .040 in (.064, .081, .102 cm) in the other
strip. Initial tests were performed to determine the drop
height necessary to produce fracture of these specimen types
and additional tests were conducted on instrumented specimens
at the necessary fracture drop height using the 12 in (30.48 cm)
long steel weight. The same fracture modes as listed previously
in Table I were observed, however the calculated fracture load
in these tests showed a decreasing trend as the thickness of the
sheet in the second strip was decreased. The complete results
of these tests are listed in Table II.

Several other combinations of sheet thicknesses were tested
using the same drop weight tester. In most all cases the trends
were the same. For a given rivet diameter as the sheet thickness
was increased, which increases bending stiffness, the rivet
fractures in shear. However, reducing the thickness of either
strip of the specimen reduces the bending stiffness and rivet/
sheet rotation occurs along with yielding of the sheet under the
bearing load with fracture then occurring by rivet shear or shear

19.

TABLE II

MAXIMUM STRESSES AND LOADS IN SPECIMENS WITH DIFFERENT THICKNESSES IN THE TWO STRIPS OF THE SPECIMENS. MS20-430-AD4 RIVET AND 2024T3 SHEET

Sheet Thickness in (cm)	Fracture Drop Ht. in (cm)	Maximum Strain, ε μ Units		Ave. Strain ($\epsilon_1 + \epsilon_2$)/2 μ Units	Ave. Max. Stress KPSI (MPa)	*Ave. Max. Load lbs.	Type of Failure
		Gage 1	Gage 2	SAME AS IN TABLE I			
.063(.160)	9.0(22.86)	636	1213	925	9.71(66.97)	612	Rivet rotation followed by rivet shear
.040(.102)	9.0(22.96)	1214	1668	1441	15.13(104.3)	605	Rivet rotation followed by rivet shear
.032(.081)	1C.0(25.40)	1502	1668	1585	16.64(114.8)	533	Slight bearing and rivet rotation followed by rivet shear
.025(.064)	11.0(27.94)	1799	1991	1895	19.90(137.2)	498	Considerable bearing and rivet shear followed by shear tear out

MS20-430-AD4

Gage 1
Gage 2
1.0(2.54)
.063(.160)

.063(.160)
.040(.102)
.032(.081)
.025(.064)
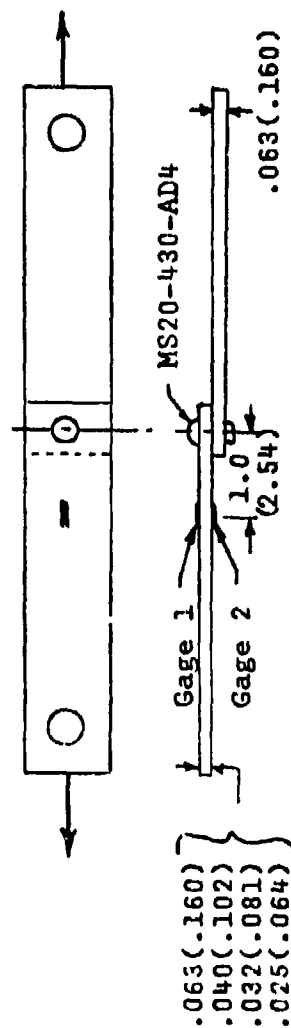
*Static shear fracture load for the rivet is 388 pounds

tear out of the sheet. As the sheet thickness is further decreased a greater drop height is found necessary to produce failure. This is due to a change in the fracture mode which requires that considerable energy must be expended to produce deformation of the sheet before fracture occurs. The higher drop height in these cases simply means more energy is available which allows for considerable deformation in the sheet to occur. It was observed that none of the specimens tested using .125 in (.32 cm) diameter rivets and 1.0 in (2.54 cm) wide sheet failed in tension across the reduced section.

Several full scale panels designed with various sizes of rivets and rivet patterns were tested in cooperation with the USAF Armament Laboratory, Eglin AFB. Details of the rivet patterns and sizes are to be incorporated in an Air Force Armament Laboratory Technical Report due to be published. Briefly the test procedure consisted of taking panels 27 in x 24.75 in (68.5 x 62.87 cm) and riveting these to a picture frame type mounting assembly .25 in (.64 cm) thick. The holder assembly was then bolted to a test stand fabricated from 1.0 in (2.54 cm) thick steel plate. The test stand was then in turn placed at the end of a fuel air explosive (FAE) chamber described in detail in Reference 6. The pressure wave from the FAE device was directed onto the plate with a known reflected pressure magnitude as obtained in previous experiments (References 6 and 7).

21.

Aluminum alloy 2024-T3 sheet with thicknesses of .05, .063 and .10 in (.127, .160, .254 cm) were used with MS20-470-AD8, MS20-470-AD6 and MS20-426-AD6 rivets. The flat plates were instrumented with strain gages as shown in Figure 10. A uniform reflected pressure of 100 psi (.69 MPa), with exponential decay in 2 milliseconds, was applied in each test run. Prior to each test, a uniform static stress in the sheet as required to produce rivet/sheet fracture was calculated, and used to predict fracture. In all cases the rivet/sheet combination as predicted to fracture by the static stress calculation fractured under the dynamic load. Also, the rivet/sheet fracture mode predicted by the static analysis was observed to cause a similar fracture under the dynamic load. The same fracture modes observed for the 1.0 in (2.54 cm) wide two strip specimens were also observed in the full scale tests. Tests results obtained for the full scale panels tested along with the analytical results will be given in the next section.

In an effort to evaluate the dynamic loading capability of some of the rivets used in the full scale tests, several variations of single lap two strip specimens were tested. For all specimens, one primary strip was held constant at .25 in (.64 cm) and three different thicknesses of .05, .063 and .10 in (.127, .160, .254 cm) were used as the second strip of the specimen. All sheet material was aluminum alloy 2024-T3 with MS20-426-AD6 rivets used for each type of specimen. As in the previous cases

22.

TOP

1 Row
MS20-470-4D8
Rivets

2 Rows
MS20-426-AD6
Rivets

2 Rows
MS20-426-AD6
Rivets

32.39

14.61

2.54

① 2 ③ 4
⑤ 6
⑨ ⑩

Panel Size
68.54x62.87cm

Strain Gages

◯ Front Mounted

▢ Back Mounted
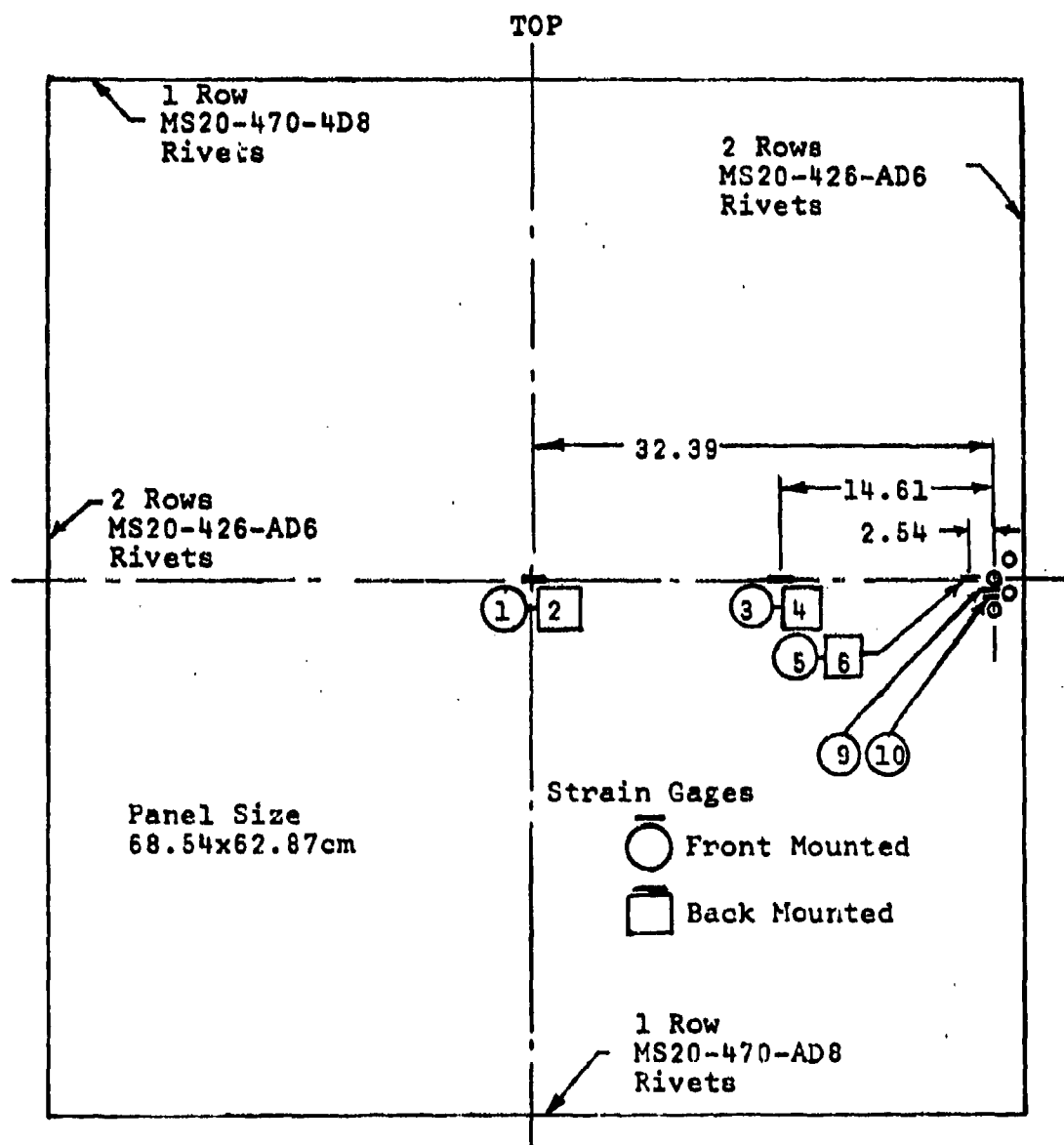
1 Row
MS20-470-AD8
Rivets

Figure 10. Rivet Arrangements and Strain Gage Positions for
Full Scale Blast Tests. Panel Dimensions in
Centimeters.

23.

noted, several uninstrumented specimens were first tested to determine the drop height necessary to produce fracture. Two instrumented specimens were tested and the strain-time history recorded. The results of these tests are given in Table III. The general observation for this set of tests was that for the thickest secondary strip tested (.1 in) the fracture mode was rivet shear with little if any noticeable sheet or rivet deformation. The .063 inch secondary strip specimen failed by rivet shear, however the drop height required for this fracture was almost three times that drop height necessary to fracture the .1 inch thick secondary strip specimen. For the thinnest secondary strip specimen (.05 in) tested using a fracture drop height of twice that of the .1 inch thick secondary strip specimen, the fracture mechanism occurring was found to be shear tear out. For the .05 inch secondary strip thick specimen severe rivet rotation and hole elongation took place before fracture.

24.

TABLE III

MAXIMUM STRESSES AND LOADS IN SPECIMENS WITH DIFFERENT THICKNESSES IN THE TWO STRIPS OF THE SPECIMENS. MS20-426-AD6 RIVETS AND 2024-T3 SHEET

Sheet Thickness in (cm)	Fracture Drop Ht. in (cm)	Maximum Strain, ε μ Units		Ave. Strain $(\varepsilon_1 + \varepsilon_2)/2$ μ Units	Ave. Max Stress KPSI (MPa)	*Ave. Max. Load Lbs.	Type of Failure
		Gage 1	Gage 2				
.1(.254)	5.5(13.97)	Broken Lead	1530	----	----	----	Rivet shear with very little deformation
.063(.160)	9.0(22.86)	792	1317	1054	11.07(76.34)	698	Bearing and elongation of hole followed by rivet shear
.05(.127)	11.5(29.21)	1500	1790	1645	17.27(119.12)	864	Severe rotation of rivet and sheet. Severe hole elongation followed by shear tear out

MS20-426-AD6

Gage 1

Gage 2

.25(.64)

1.0

2.50

$\left.\begin{array}{l}.10(.254)\\.063(.160)\\.05(.127)\end{array}\right\}$
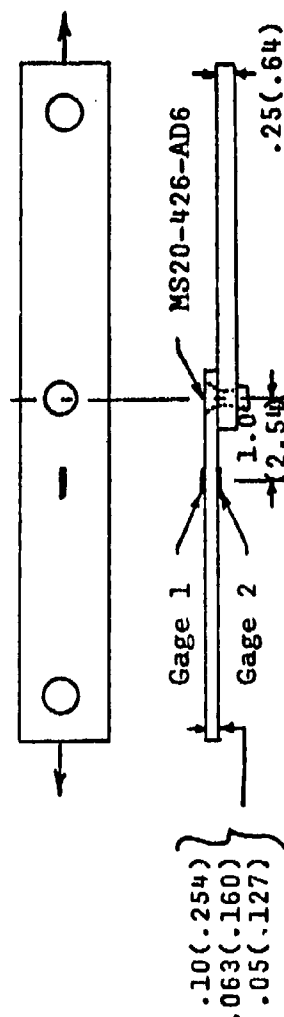
*Maximum static shear load 862 pounds

25.

SECTION III

THEORETICAL ANALYSIS OF FULL SCALE TESTS

The stress analyses of the full scale test panels were accomplished using the computer code DEPROP (Dynamic Elastic Plastic Response of Panels, Reference 8). This code has an elastic-plastic option, however for ready use all boundaries must be simple, clamped or combinations thereof. There is no accomodation for variations of stiffness or elasticity at the boundaries. Analyses of plates as used in the full scale tests were performed for a symmetrical flat aluminum plate using the following set of input.

Material: 2024-T3 aluminum

Elastic modulus: 10.5×10^6 PSI (72.4GPa)

Strain hardening modulus: $.147 \times 10^6$ PSI (.101GPa)

Plate Sizes: 27x24.75x.1 in (68.58x62.87x.254 cm)

27x24.75x.063 in (68.58x62.87x.160 cm)

27x24.75x.05 in (68.58x62.87x.127 cm)

Loading: Uniformly distributed $P = P_{max}(1-t/\tau)\exp(-\alpha t/\tau)$

where: P_{max} = 100 PSI(.69MPa)

$\tau = 2.05 \times 10^{-3}$ sec

Boundary conditions: Both clamped all edges and simply supported all edges cases were evaluated for the three plate thicknesses.

In keeping with conventional methods of defining boundary loads in force/unit length, the front and back plate stresses, normal and one inch from the boundary, were averaged to obtain a membrane stress and then multiplied by plate thickness to give a force/unit length. The load distributions found one inch from the edge by the theoretical analysis were found to very closely approximate the load distribution at the edge. Only the normal stresses were considered as important along the boundary since the calculated tangential or shearing stresses close to the mid point of the boundary are negligible in comparison to the normal stresses. This was also verified experimentally in the full scale tests with the strain gages aligned parallel to the edge of the plate.

The strains monitored one inch from the plate edge were converted to an equivalent for. ./unit length by using a constitutive relation for membrane stresses. The analytical results obtained for both clamped and simple supports and experimental results for all three plate thicknesses tested are shown in Figures 11, 12 and 13.

These figures show that the analytically determined boundary loads for clamped or simply supported plates reach a maximum at about 0.5 millisecond whereas the maximum experimental value reaches a maximum at about 1.0 millisecond. The analytical/experimental differences as noted are assumed to be related to

27.

Figure 11. Distributed Normal Load Vs Time for A Point One Inch From Edge of Rivet Line at the Midpoint of the Side of Panel Shown in Figure 10. (Gage Positions 5 and 6) Panel Thickness 0.10 (.254).

28.

Figure 12. Distributed Normal Load Vs Time for A Point One Inch From Edge of Rivet Line at Midpoint of the Side of the Panel Shown in Figure 10. (Gage Positions 5 and 6) Panel Thickness 0.063 in (0.160 cm).
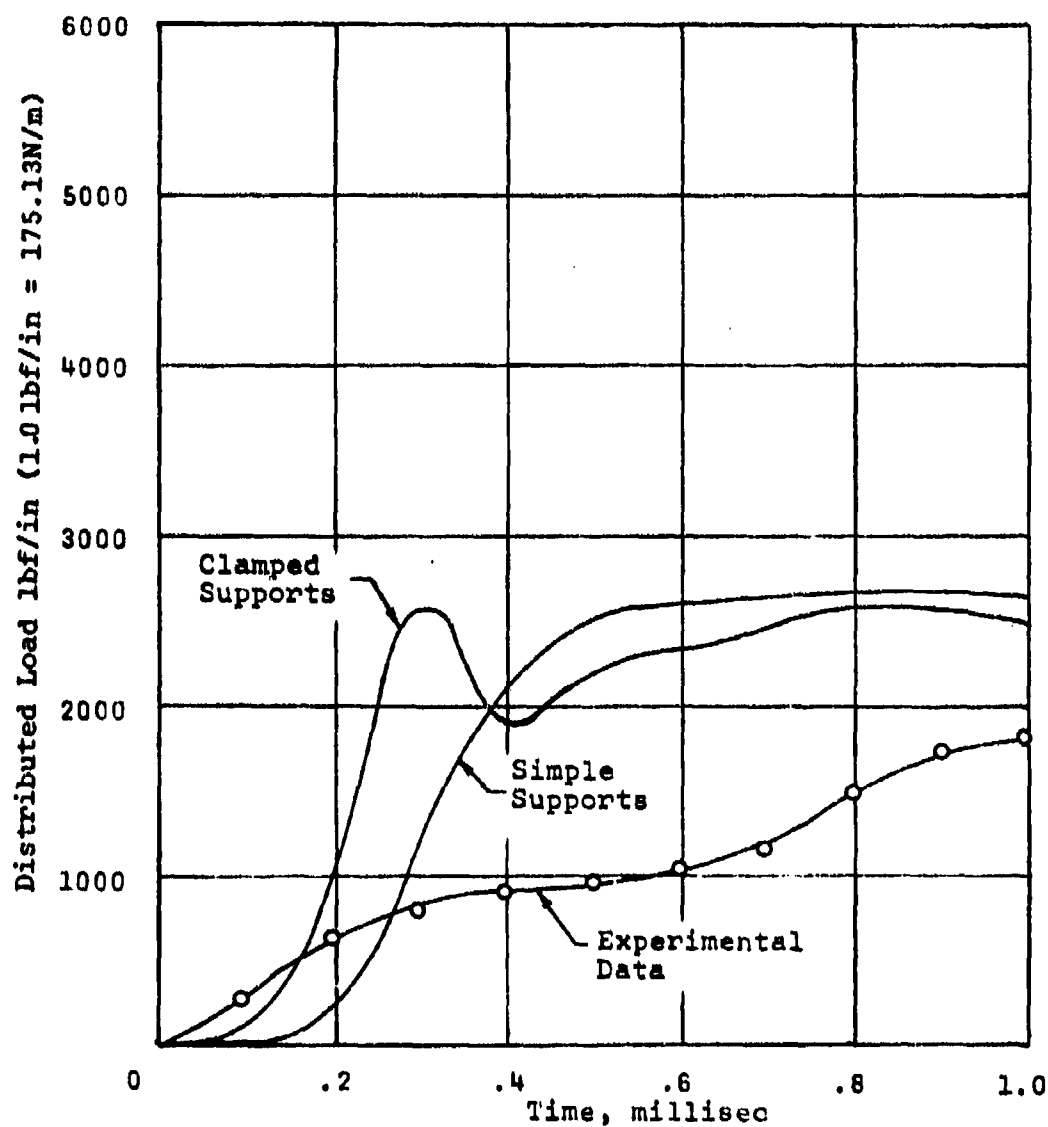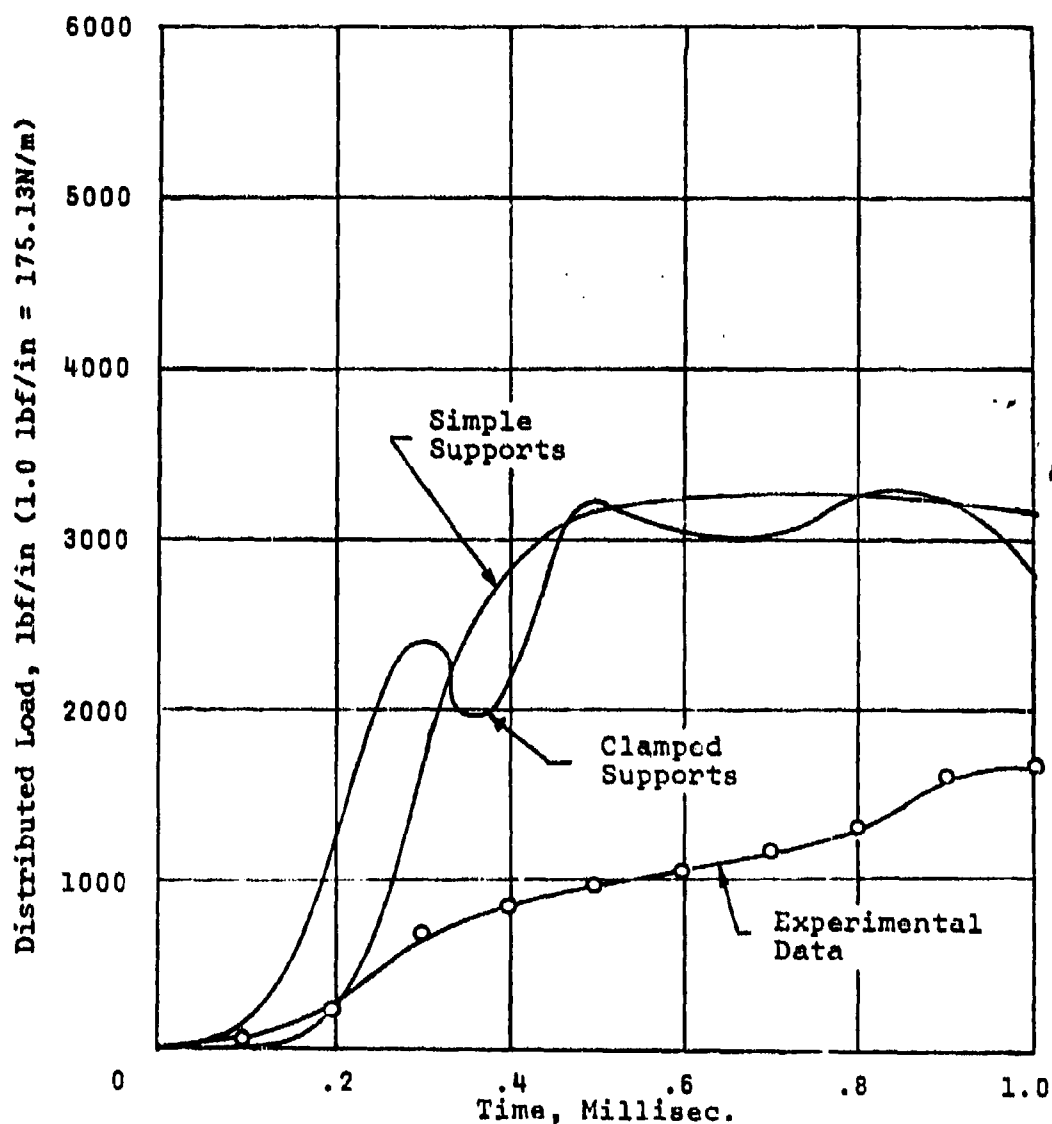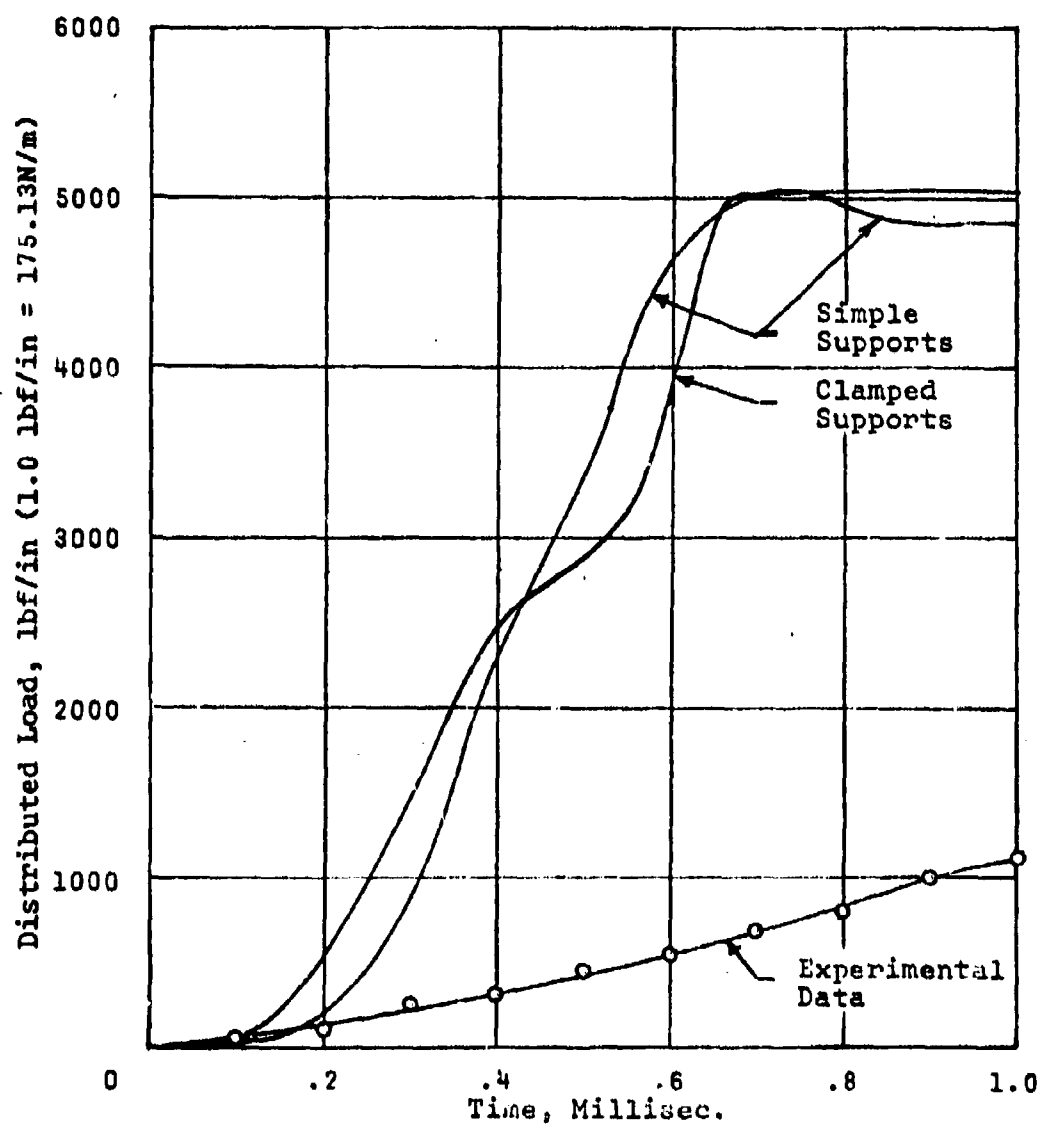
29.

Figure 13. Distributed Normal Load Vs Time for A Point One Inch
From Edge of Rivet Line at Midpoint of the Side Panel
Shown in Figure 10. (Gage Positions 5 and 6) Panel
Thickness 0.10 in (.254 cm).

30.

differences in the plate boundary stiffness. For stiff boundaries the stresses tend to build up faster than at less stiff boundaries. For full scale tests with much stiffer boundaries, such as the simulated clamped edges of Reference 7 the plates were found to fail along the edges at about 0.5 millisecond for loads similar to those of this study.

The stresses calculated analytically based on a fully clamped/ rigid boundary are expected to be even larger than those of the less stiff boundaries. Harris and Ojalvo (Reference 9) show that for riveted boundaries, with a given rivet diameter to sheet thickness, as the ratio of the rivet modulus to the sheet stiffness decreases the maximum stress at the rivet boundary increases. In addition changes in sheet and boundary stiffness will produce additional changes in both the failure and fracture modes.

For the riveted plate boundary using MS20-426-AD6 rivets, the rivet line consisted of two rows of staggered rivets spaced equally 1.25 in (3.18 cm) along each line giving a boundary of 2 rivets per 1.25 inches or a rivet spacing of 1.6 rivets/inch. The dynamic rivet fracture loads identified in Table II are determined for 1.0 in (2.54 cm) wide specimens, therefore a factor of 1.6 times these indicated loads would be necessary to fracture the full scale tests attachments. For the full scale plate tested, this gives a boundary fracture load of approximately 1117 pounds/inch for .063 in (.16 cm) thick plate and 1383

pounds/inch for the .05 in (.13 cm) thick plate. The experimental
results of the full scale tests show an approximate fracture load
of 1800 pounds/inch for the .05 inch plate and approximately 1700
pounds/inch for the .063 inch plate. These results and comparisons
are premised on the assumption that the 100 psi (.69MPa) blast
load causes fracture of the rivets and that approximately half
the experimental tests result in fracture and the other half
cause severe rivet rotation and rivet hole elongation.

SECTION IV

GENERAL DISCUSSION AND CONCLUSIONS

4.1 DISCUSSION

In summary, taking into consideration the over 250 dynamic
tests run, the dynamic fracture modes of riveted joints were
found to be essentially the same as those found in statically
loaded riveted joints. Basically, for a given rivet type and
diameter, with variations in sheet thickness, as the sheet thick-
ness decreases below that required for dynamic rivet shear a change
in fracture mode occurs. Combinations of several fracture modes
can appear with decreasing sheet thicknesses until tensile sheet
fracture occurs between the rivet holes. For thicknesses above
that necessary to produce sheet fracture between rivets, severe
rivet and sheet rotation occurs and fracture can occur as rivet
shear or shear tear out of the sheet.

Examination of flat panel tests run on full scale aircraft,
show rivet shear or what appears to be the two kinds of sheet
failure as shown in Figure 14. However, further observation and
examination of single rivet tests indicates that a scalloped
fracture (Figure 14a) occurs. This is the result of a crack
formation developing at the sides of the hole which is then torn
out by shearing action of the large rivet rotation proceeding and
following the initial crack formation. The large rivet rotation
in most cases is preceeded by hole elongation and the net section

33.
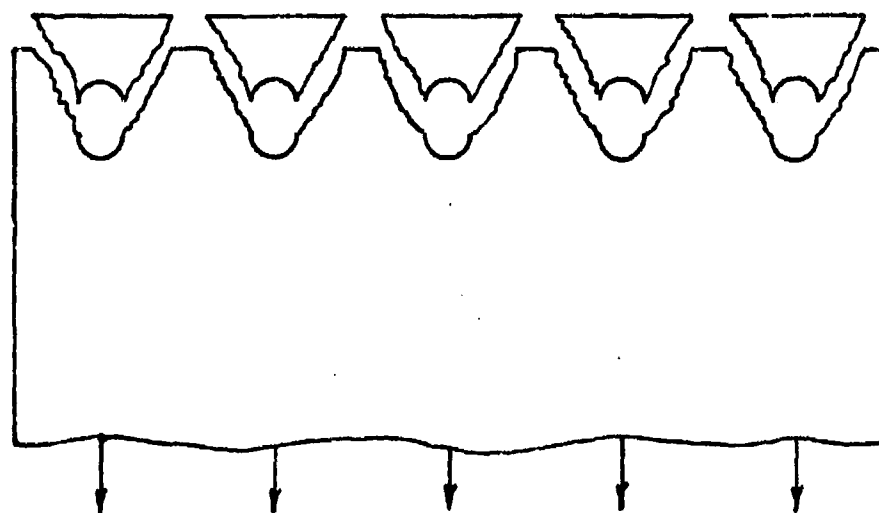
a) Scalloped Fracture
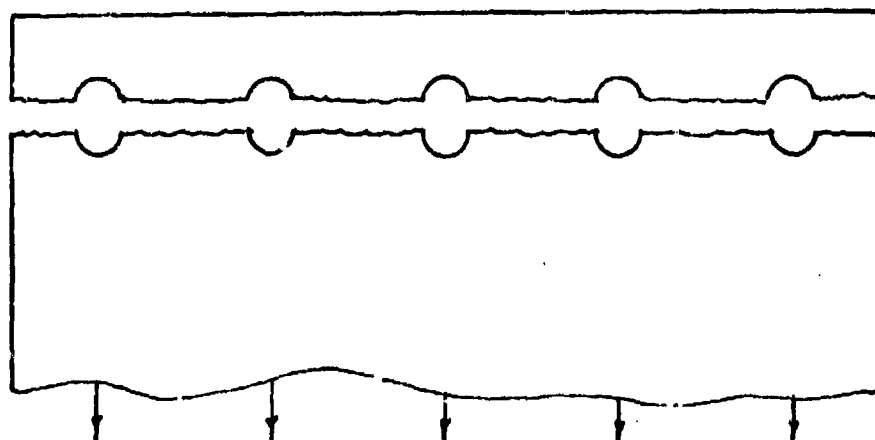
b) Net Section Fracture

Figure 14. Appearance of Sheet Fracture for Riveted Joint
Resulting from Blast Load.

34.

stress between the rivets appears to never reach the ultimate stress of the material. For very thin sheets the driving force necessary for fracture is the net tensile stress between the rivets. Once the crack has formed at the edges of the hole catatrosphic or elastic type fracture will occur. This elastic type fracture is brought about by the transition from a Mode I plane strain fracture to a plane stress shear rupture with decreasing plate thickness as discussed by Irwin (Reference 10). Below a critical thickness of 0.5 in (1.27 cm) for 2024-T4 aluminum (Reference 11) the fracture toughness decreases with decreasing sheet thickness and as a result when a crack of sufficient length forms, failure or fracture occurs catastrophically. However, in dynamic loadings the driving force or stress may occur over a shorter time period and the tension failure between rivets can occur only over a very short distance. In addition, brittle type sheet failure has a tendency to occur for 7075 aircraft aluminum due to the higher yield stress and lower elongation as compared to the more ductile 2024 aluminum series.

For prediction purposes, of when riveted joints fail under dynamic loads there appears to be no readily available analysis for use. In order to establish a dynamic analysis model a joint stiffness is essential, since the build up of stress in the rivet/ sheet element is governed by the response of the rivet/sheet combination to the applied load. Harris and Ojalvo (References 9 and

12) used a finite element code to calculate static joint stiff-
nesses and their analytical results when compared with experiment
showed good correlation. Since there is very little strain rate
sensitivity found in cold worked aluminum alloys it is expected
that statically determined joint stiffnesses could be used with
good success in calculating joint response under dynamic loads.

4.2 CONCLUSIONS

1. Dynamic stress concentrations associated with holes and
riveted joints are approximately equal to the static stress con-
centrations.

2. Fracture/failure modes of riveted joints subject to dynamic
loads are essentially the same as those for riveted joints when
subjected to static loads.

3. Dynamic rivet/sheet response, failure and fracture are
very dependent on the joint stiffness and applied load-time
history.

4.3 RECOMMENDATIONS

1. Run a continued test series on tensile rivet sheet com-
binations with strain gage instrumentation to determine loading
history and time to fracture.

2. Continue static rivet sheet tests in various combinations
to determine joint stiffnesses to be used in dynamic response
methods using finite element codes similar to the static methods

of Reference 11. Alternatively, a modification of the boundary conditions to accomodate variable boundary stiffnesses in the code of Reference 9 are recommended.

3. Continue full scale tests on flat and curved panels with strain gage instrumentation to verify methods of 2 and 3 above.

SECTION V

REFERENCES

1. Timoshenko, S. P., and Goodier, J. N., Theory of Elasticity, McGraw Hill Book Co., Third Ed., 1970.

2. Peterson, R. E., Stress Concentration Factors, J. Wiley and Sons, 1974.

3. Durelli, A. J., and Dally, J. W., "Stress Concentration Factors Under Dynamic Loading Conditions," J. Mech. Eng. Sci., Vol. 1, No. 1, pg. 1-5, 1959.

4. Dally, J. W., and Halbleib, W. F., "Dynamic Stress Concentrations at Circular Holes in Struts," J. Mech. Eng. Sci., Vol. 7, No. 1, pg. 23-26.

5. Mil Handbook 5.

6. Ross, C. A., and Strickland, W. S., Response of Flat Plates Subject to Mild Impulsive Loads," Bulletin 45, Shock and Vibration Information Center, pg. 105-116, 1975.

7. Strickland, W. S., and Ross, C. A., "The Plastic Response of Rectangular Membrane Plates to Mild Explosive Loading Functions," U. S. Air Force Armament Lab., Eglin AFB, FL, AFATL-TR-74-181, 1974.

8. Mente, L. J., and Lee, W. N., "DEPROP - A Digital Computer Program for Predicting Dynamic Elastic-Plastic Response of Panels to Blast Loadings," U. S. Air Force Armament Lab, Eglin AFB, FL, AFATL-TR-76-71, 1976.

9. Harris, H. G., and Ojalvo, I. V., "Simplified Three-Dimensional Analysis of Mechanically Fastened Joints," Proceedings of the Army Symposium on Solid Mechanics, pg. 177-192, 1974.

10. Irwin, G. R., J. Basic Engineering (Trans. ASME), 82D, 417 (1960).

11. Tetelman, A. S., and McEvely, Jr., Fracture of Structural Materials, J. Wiley & Sons, 1967.

12. Harris, H. G., Ojalvo, I. V., and Hooson, R. E., "Stress and Deflection Analysis of Mechanically Fastened Joints," U. S. Air Force Flight Dynamics Lab., Wright-Patterson AFB, Ohio, AFFDL-TR-70-49, 1970.